Hindawi
Advances in Materials Science and Engineering
Volume 2022, Article ID 1844556, 10 pages
https://doi.org/10.1155/2022/1844556

Research Article

Study on Damage of the OGFC Mixture Based on Characteristics of Void Distribution

Teng Xu-qiu, Zhao Dongdong, and Zhang Fuqiang

College of Civil Engineering, LanZhou JiaoTong University, Box 15, Lanzhou, Gansu, China

Correspondence should be addressed to Teng Xu-qiu; tengxuqiu@mail.lzjtu.cn

Received 18 November 2021; Revised 25 February 2022; Accepted 26 February 2022; Published 24 May 2022

Academic Editor: Andrea Petrella

The void distribution characteristics of the drainage asphalt mixture have a certain influence on its durability. In this paper, X-ray CT technology and digital image processing technology are used to study the void distribution characteristics of three different graded asphalt mixtures, and the void ratio, void quantity, void equivalent diameter, and void fractal dimension of drainage asphalt mixtures are determined. On this basis, the damage characteristics of the asphalt mixture are analyzed with the split strength as the index, and the relationship between the void fractal dimension and the split strength is established. The relationship between the void diameter and the durability of the OGFC mixture is determined by the influence of the void diameter on the void fractal dimension. The results show that the void distribution characteristics of the OGFC mixture have a significant impact on its durability. The void larger than 3 mm in OGFC asphalt mixture has a greater impact on the durability of asphalt mixture. Even if the void ratio of different OGFC mixtures is relatively close, its durability is also very different. The difference in durability is mainly due to the difference of the void structure and the proportion of the number of large voids above 5 mm.

1. Introduction

With the development of computer technology and digital image processing technology, it is possible to obtain the internal structure of the asphalt mixture [1–6]. Digital image processing (DIP) is used to extract interesting objectives, so the influence of microstructure on asphalt mixture can be investigated [7–14]. Using digital image processing technology, researchers can process slice images taken by CT scans or high-definition cameras and distinguish the materials according to the different CT values and colors on the images, so as to obtain a clear and detailed structure diagram. It can provide reference for studying its internal structure characteristics and distribution law. Many researchers have applied nondestructive evaluation by using X-ray computed tomography (CT) to assess civil engineering materials [15, 16]. The internal structure and voids distribution of the asphalt mixture were achieved by X-ray CT [17, 18]; Masad.2002 [19–21].

Masad et al. quantitatively analyzed the effect of the compaction method on the internal structure of asphalt mixture samples by using digital camera technology and CT technology. By changing the conditions of rotary compaction to make it close to the level of on-site compaction, the compaction effect was finally evaluated. The results show that different compaction methods lead to different internal void distribution rules in the asphalt mixture, and the void ratio at the upper and lower ends of the asphalt mixture specimen is greater than the void ratio in the middle [18]; Masad et al. [22, 23]. Torres et al. studied the effect of pore distribution in HMA on its water permeability by CT scanning technology [24]. They found that Lognormal and Weibull distribution models can effectively fit the relationship between pores and water permeability, and a better correlation between connected pores and water permeability has been found. Through CT scanning and image processing of specimens with the same volume parameters such as VCA and VMA, Xu et al. [25] found that with different internal pore distributions of the specimens, the permeability and moisture damage were also different. Therefore, the pore distribution parameter as the evaluation index of water stability is more sensitive than the traditional volume parameter. Zhang Jialin used CT technology to analyze the horizontal and vertical void ratio, void equivalent diameter, void fractal dimension, and other parameters of

asphalt mixture specimens [26]. The research results showed that the void equivalent diameter was mainly distributed between 3 mm and 9 mm. The transverse percentage of voids of the mixture specimen is greater than the longitudinal percentage of voids, that is, the transverse drainage capacity is better than the longitudinal drainage capacity. Wu Wenliang of the South China University of Technology processed the CT slices of the asphalt mixture samples to obtain digital images that could characterize the void characteristics of the asphalt mixture and analyzed the plane and spatial distribution characteristics of the asphalt mixture [27].

In summary, many research studies have been conducted on the internal structure or loss of performance of the asphalt mixture in the past decades, but few studies have paid attention to comprehensive consideration of the relationship between void structure and performance evolution of the OGFC mixture from the meso and macro levels. Therefore, this paper uses CT scanning technology to explain the difference of indirect tensile strength of OGFC mixtures with different void structures, so as to realize a multiscale characterization of the damage characteristics of the OGFC mixtures. Finally, the relationship between void fractal dimension and splitting strength of OGFC mixture is established, and the void characteristics of the OGFC mixture with serious damage are determined.

2. Materials and Methods

2.1. Sample Preparation. In order to study the void distribution characteristics of the asphalt mixture, the drainage asphalt mixture (OGFC-13) with large void characteristics was selected as the research object, and the specimen was molded by the Marshall method. The specimen size was $\Phi 101.6\,\text{mm} \times 63.5\,\text{mm}$. The volumetric method was used to determine the void ratio of the asphalt mixture specimen and calculate the connected void ratio of the asphalt mixture specimen.

2.2. Materials. The coarse and fine aggregates used in this research were all basalt, and the ore powder was milled from limestone. The rubber asphalt was used as the binder, and fiber was mixed into the OGFC-13 mixture. The technical indicators of the raw materials are shown in Tables 1–4.

2.3. Mineral Material Grading Design. Since the percentage of voids of OGFC is closely related to the pass rate of the 2.36 mm sieve, the target percentage of voids of OGFC is controlled by adjusting the pass rate of the aggregate at the 2.36 mm sieve. First the gradation is determined according to the median value of the gradation recommended by the specification OGFC-1, then OGFC-2 and OGFC-3 are close to the upper and lower limits of the recommended gradation specifications. The pass rate of the three groups of mixture grading in each sieve is shown in Table 5.

2.4. Void Ratio and Connected Void Ratio Calculation. Table 6 shows the calculation results of the void ratio and connected void ratio of the three OGFC mixtures.

3. Results and Discussion

The void distribution characteristics of asphalt mixture specimens are affected by many factors such as molding method, aggregate gradation, uniformity of reclaiming, and molding temperature. This study intends to investigate the distribution of void ratio and void quantity at different heights of OGFC specimens, the void gradation and void fractal dimension of different gradation asphalt mixtures, and the distribution of void equivalent diameters at the cross section of the specimen. The void distribution characteristics of OGFC materials are studied.

3.1. Percentage of Void Distribution. According to the results of CT scanning, the gray threshold value T_1 of the CT scanning image is adjusted first, and then the gray value of pixels on the image is normalized. The gray value greater than T_1 is set to 255, and the gray value less than T_1 is set to zero. The result of image processing after binarization is shown in Figure 1, based on which the number of voids and void ratio of each two-dimensional slice can be determined.

Using MATLAB program to count the scanning slices of OGFC mixture, the total number of pixels in the circular part in Figure 1 is 32679, and the total number of pixels in the black part outside the circle is 12475. The difference between the sum of black pixels in the entire quadrilateral and the black pixels outside the circle is the number of black pixels in the circle, and the ratio of the difference to the total number of pixels in the circle is the void ratio of the scan slice. It can also determine the percentage of voids of the entire specimen.

It can be seen from Figure 2 that the percentage of voids of the OGFC mixture shows a C-type distribution along the height of sample. The void ratio decreases from both ends to the middle. The percentage of voids at both ends of the test sample is larger because the interpolating effect on the mixture causes more coarse aggregate and less fine aggregate at the end of the test simple when the test sample is formed. The measured percentage of voids values and the calculated percentage of voids values from image statistics of OGFC-1~OGFC-3 are shown in Table 7. The CT scan interval used in this study is 0.5 mm. It can be seen that the void ratio calculated from the scanned image is very close to the measured void ratio from Table 7.

Masad found that the void ratio at the upper and lower ends of the asphalt mixture specimen is greater than the void ratio in the middle [18, 23, 28]. This means that the distribution of void ratio along the height of sample for the normal asphalt mixes studied by Masad is basically the same as that of the OGFC mixtures.

3.2. Number of Void Distribution. The void distribution inside the asphalt mixture has a great influence on the performance of the asphalt mixture. In this paper, with the help of Image-Pro Plus's image processing and analysis functions, the number of voids, equivalent diameter distribution of voids, and void fractal dimensions in different gradation types of OGFC mixture samples are counted in

Table 1: Properties of coarse aggregate.

Test items		Test method	Unit	Normative value	Measured value
Polished stone value		T0312	BPN	≥38	58
Content of needle or plate	>9.5 mm	T0312	%	≤15	12.3
	<9.5 mm	T0312	%	≤20	16.4
Water absorption		T0304	%	≤3.0	1.7
Apparent density		T0304	$g{\cdot}cm^{-3}$	≥2.50	2.734
Crushing value		T0316	%	≤28	18.9
Adhesion		T0316	Level	≥4	4
Los Angeles wear value		T0317	%	≤30	15.3

Table 2: Properties of fine aggregate.

Test items	Test method	Unit	Normative value	Measured value
Sand equivalent	T0334	%	≥50	63.9
Angularity	T0345	s	≥30	36.1
Apparent density	T0328	g·cm-3	≥2.450	2.771
Methylene blue value	T0349	g·kg	—	20
Mud content(<0.075 mm)	T0333	%	<5.0	2.79
Robustness (>0.3 mm)	T0340	%	—	12.0

Table 3: Properties of rubber asphalt.

Test items		Test method	Unit	Normative value	Measured value
Penetration at 25°C		T 0604	0.1 mm	40~80	61
Ductility at 5°C		T 0605	cm	>10	17.3
Thin film oven test	Ductility at 5°C	T0605	cm	≥5	15.9
	Penetration ratio at 25°C	T0604	%	≥60	94.8
	Quality loss	T0609	%	≤±0.1	0.2
Elastic recovery		T0615	%	>55	71.5
Rotational viscosity at 180°C		T0625	Pa.s	1.0~4.0	1.64

Table 4: Properties of mineral powder.

Test items		Test method	Unit	Normative value	Measured value
Plasticity index		T0354	-	<4	3.6
Apparent density		T0352	$g{\cdot}cm^{-3}$	≥2.5	2.679
Stability		T0355	-	Measured	No change in color after heating
Hydrophilic coefficient		T0353	-	<1	0.6
Exterior		-	-	No clumps	No clumps
Particle size range	<0.6 mm	T0351	%	90–100	100
	<0.3 mm		%	75–100	95.2
	<0.075 mm		%	100	85.9

Table 5: Gradation composition.

Composite gradation	Passing percentage of each sieve (%)									
	16	13.2	9.5	4.75	2.36	1.18	0.6	0.3	0.15	0.075
OGFC-1	100	94.1	70.2	21.0	16.4	12.2	8.0	5.9	5.1	4.5
OGFC-2	100	92.5	62.4	18.7	14.8	11.2	7.6	5.8	5.1	4.5
OGFC-3	100	91.5	61.4	16.8	13.1	10.1	7.1	5.6	5.0	4.4
Upper limit of gradation	100	100	80	30	22	18	15	12	8	6
Median gradation	100	95	70	21	16	12	9.5	7.5	6	4
Lower limit of gradation	100	90	60	12	10	6	4	3	4	2

Table 6: OGFC mixture's percentage of voids and connected percentage of voids (%).

Specimen number	1		2		3		4	
Void category	Percentage of voids	Connected percentage of voids	Percentage of voids	Connected percentage of voids	Percentage of voids	Connected percentage of voids	Percentage of voids	Connected percentage of voids
OGFC-1	20.4	14.0	19.0	15.2	20.6	14.9	21.6	17.0
OGFC-2	20.3	15.8	21.3	17.6	20.6	15.8	21.5	18.0
OGFC-3	22.8	19.9	23.0	20.2	23.9	21.9	23.9	21.2

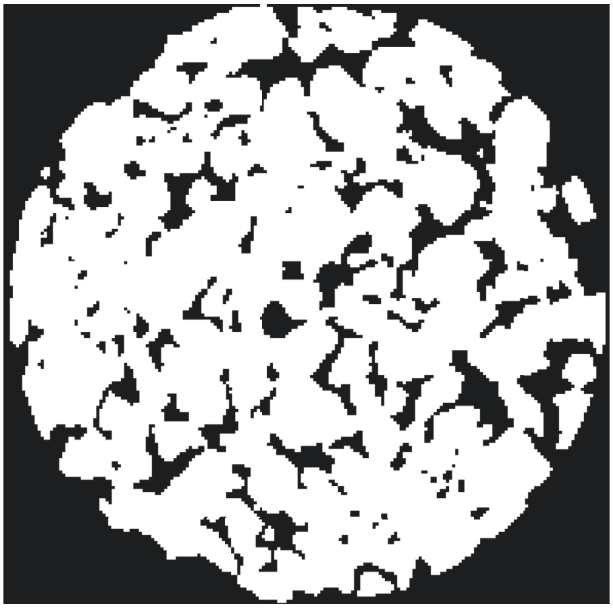

Figure 1: Binarization diagram of a bituminous mixture sample.

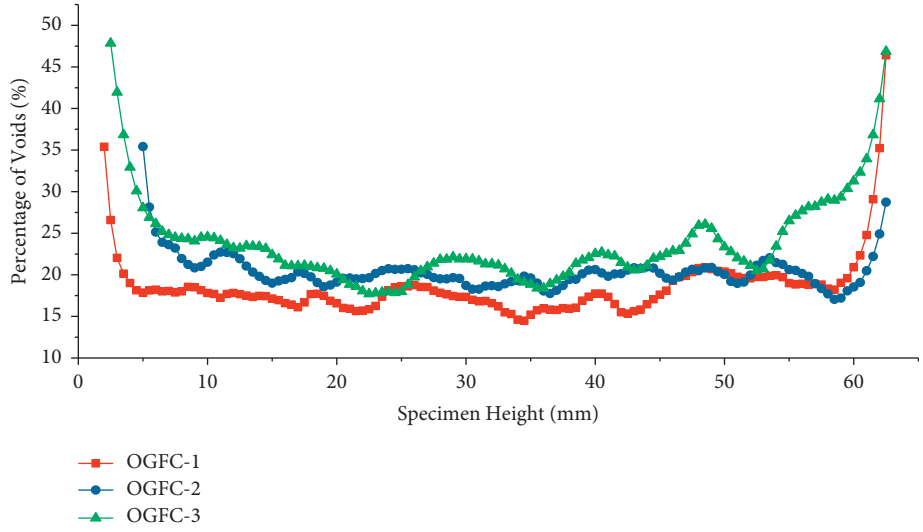

Figure 2: Percentage of void distribution along the height of the specimen.

Table 7: Measured percentage of voids and calculated percentage of voids.

Gradation	Measured percentage of voids	Calculated percentage of voids	Difference
OGFC-1	19.0	18.6	0.4
OGFC-2	20.3	20.4	0.1
OGFC-3	23.9	23.8	0.1

batches. The change in the number of voids along the height of the specimen is shown in Figure 3.

It can be seen from Figure 3 that the number of voids in the OGFC mixture shows a convex distribution along the height of samples. The number of voids increases from both ends to the middle. The number of voids at both ends of the test samples is small, while the number of voids in the middle is relatively large. Combining with the percentage of void distribution of Figure 2, it can be seen that the void volume at both ends of the specimen is large and the number is small, while the void volume in the middle of the specimen is small and the number is large.

3.3. Void Equivalent Diameter Distribution. The equivalent diameter of the void can represent the size of the void inside the asphalt mixture. The distribution law can be clarified by counting the size distribution of the equivalent diameter. By comparing and analyzing the void equivalent diameter distribution curves of different grades of OGFC mixtures, the durability of OGFC mixtures with different grades could be evaluated. The distribution of the equivalent diameter of the voids of OGFC-1~OGFC-3 mixtures is shown in Figures 4–7.

From Figures 4–6, it can be seen that the distribution range of the equivalent diameter of OGFC mixture voids is roughly between 0 and 10 mm, and most of the voids are distributed in the range of 1~4 mm, accounting for about 70%. The results are very close to those of [29]. Their research results shows voids with 0~4 mm equivalent aperture account for the largest proportion in the open-graded asphalt mixture. The space of 0~1 mm accounts for about 10%, and the space of more than 4 mm is about 20%. This part of the large void is mainly distributed on the surface of the asphalt mixture specimens. In the OGFC-1 and OGFC-2 mixture samples, the voids of 1 to 2 mm are the most prevalent, and their proportions reach 32.5% and 29%, respectively. In OGFC-3, the void of 2 to 3 mm is the most common, accounting for 23%. It can be seen from Figure 7 that the air-diameter frequency distribution functions of OGFC-1 and OGFC-2 mixtures are relatively close, and they are basically the same in the range of 1 to 5 mm. OGFC-2 has a wider range of void diameter distribution than OGFC-1, but the excess part occupies a smaller proportion and is mostly distributed on the surface of the specimen. The OGFC-3 mixture has more voids larger than 3 mm, so the durability order is OGFC-2>OGFC-1>OGFC-3. In summary, combined with the measured interconnected void fraction in Table 3, the drainage capacity order is: OGFC-3>OGFC-2>OGFC-1. Taking a comprehensive consideration, it is more reasonable to select OGFC-2 gradation.

3.4. Void Gradation Analysis. In this paper, the void gradation is the size distribution of the equivalent diameter of the void and mainly refers to the distribution ratio of the void diameter of different sizes. Under the combined action of internal and external causes, as the skeleton structure of asphalt mixture changes, its void distribution will be affected, and the void gradation will also change. Figure 8 shows the void gradation diagram of OGFC-1~OGFC-3 mixture samples.

It can be seen from Figure 8 that the overall size distribution of the void diameter is: OGFC-1 < OGFC-2 < OGFC-3. As the optimal gradation of OGFC-2, its gradation is close to the S-type distribution, that is, most of the voids are concentrated in the middle of the void diameter range, and there are fewer particularly large and small voids.

3.5. Void Fractal Dimension. In order to characterize the complexity of the void structure of OGFC mixture, the fractal dimension in fractal geometry is introduced to illustrate the structural characteristics of the void. Commonly used methods of geometric fractal dimensions are the number box method [30], the variable size method, and the small island method. In this paper, the box-counting method is used to study the characteristics of the gap fractal dimension. This method is commonly used to calculate the fractal dimension of complex irregular graphics, and a square box with a variable length of r is used to cover the fractal dimension of the graphics. Due to the irregularity of the covered graphics, there are often many holes and cracks that are not covered or part of it is covered. Count the number of these nonempty boxes, and record the number of nonempty boxes as $N(r)$, and then reduce the size of the box, and then calculate the new $N(r)$. When $r \longrightarrow 0$, the fractal dimension defined by the box method is obtained as follows:

$$D_0 = -\lim_{T \longrightarrow 0} \frac{\lg N(r)}{\lg r}. \tag{1}$$

In practical applications, a series of r and $N(r)$ can be obtained first, and then a straight line can be determined in the double logarithmic coordinate lgN-lgr, and the slope is D_0. Figure 9 shows the fractal dimensions of four different rules and smoothness graphs.

An OGFC mixture sample has more than 130 CT slices. In order to obtain the fractal dimension of the entire specimen, first obtain the void fractal dimension of each slice, and then calculate the average value to obtain the void fractal dimension of the entire specimen. The calculation formula is shown in (2), and the fractal dimension of OGFC1~OGFC3 mixture is shown in Figure 10.

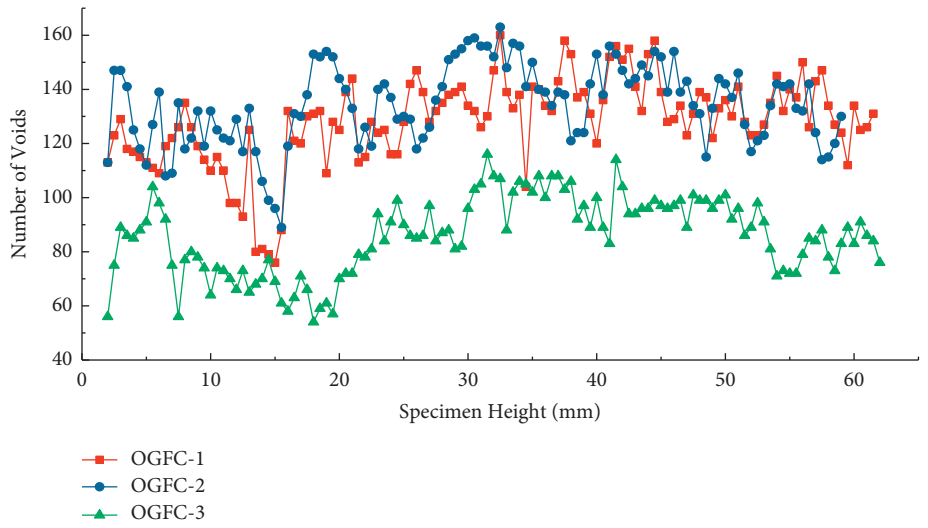

Figure 3: Distribution of the number of voids along the height of the specimen.

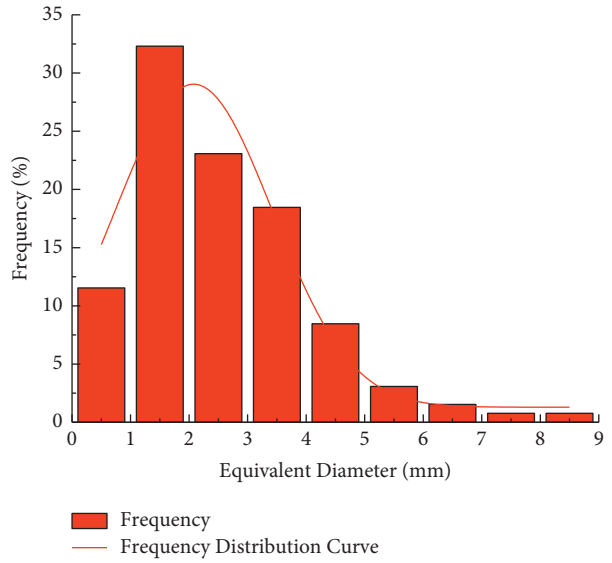

Figure 4: Equivalent diameter of OGFC-1.

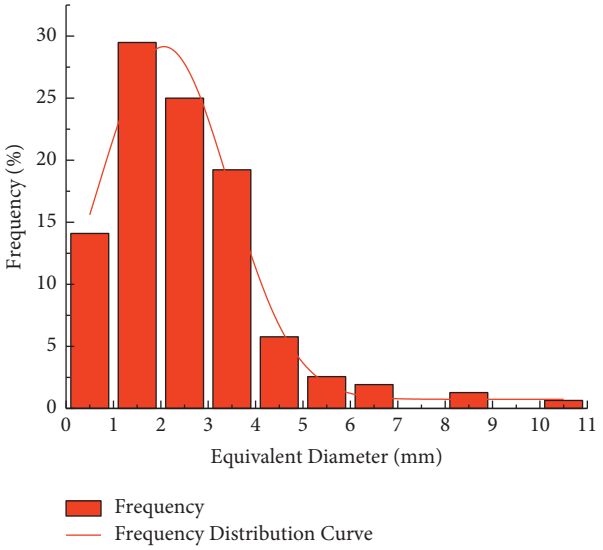

Figure 5: Equivalent diameter of OGFC-2.

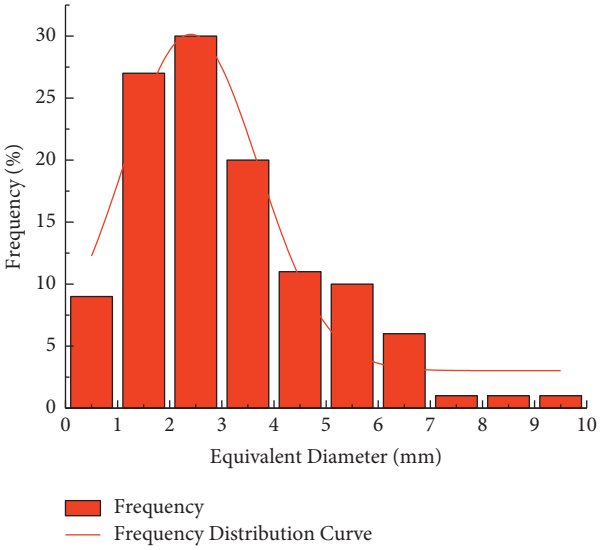

Figure 6: Equivalent diameter of OGFC-3.

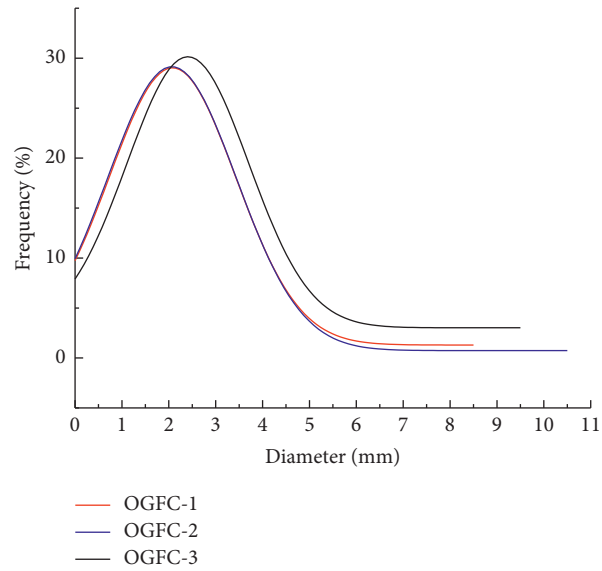

Figure 7: Frequency distribution function of the void diameter of three kinds of specimens.

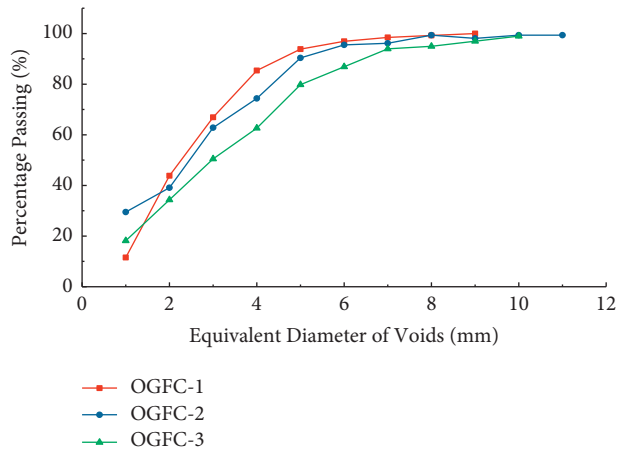

Figure 8: Void gradation diagram.

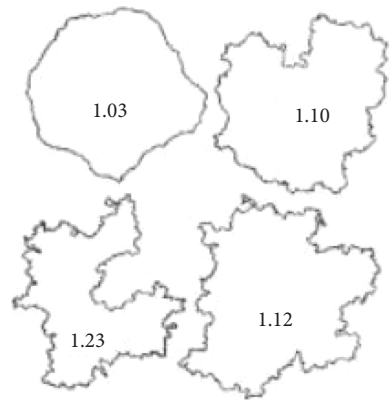

Figure 9: Fractal dimensions of four different rules and smoothness graphs.

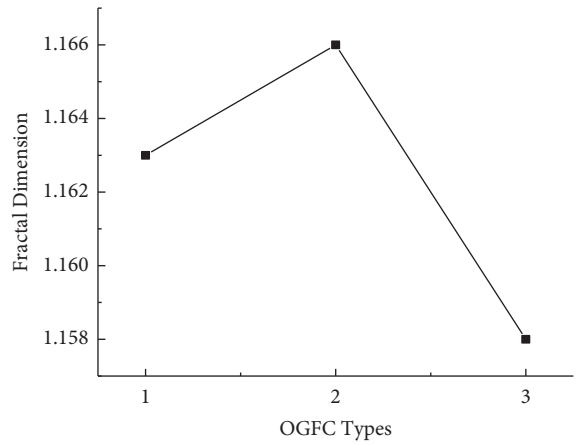

Figure 10: Fractal dimension distribution of different types of OGFC.

Table 8: Splitting strength of different gradation specimens.

Gradation	Percentage of voids	Void fractal dimension	Number of voids	Splitting strength (MPa)
OGFC-3	23.9	1.58	86	0.49
OGFC-1	19.0	1.63	128	0.64
OGFC-2	20.3	1.66	134	0.71

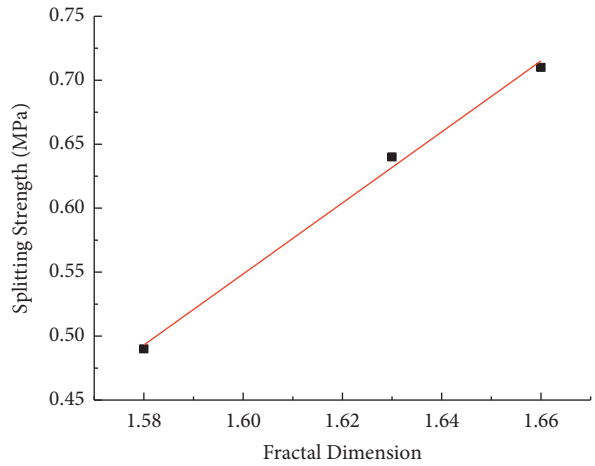

Figure 11: Relationship between the splitting strength and void fractal dimension.

$$D = \frac{\sum_{i=0}^{n} D_i}{n}, \tag{2}$$

where D is the fractal dimension of voids in the asphalt mixture and n is the number of CT image slices of the asphalt mixture.

3.6. Influence of Void Distribution Characteristics on Splitting Strength of Asphalt Mixture. The splitting strength of OGFC mixture is closely related to the void distribution. Related research shows that the splitting strength can indirectly reflect the ability of asphalt mixture to resist fatigue damage and water damage. In this paper, we will study the effect of void distribution characteristics on the splitting strength of OGFC mixture according to the void ratio, void fractal dimension, void number, and void equivalent diameter obtained above. In this paper, three gradations of OGFC-1, OGFC-2, and OGFC-3 were molded to measure the splitting tensile strength. Some of the measurement results are shown in Table 8.

It can be seen from Table 8 that the porosity of the OGFC-2 specimen is greater than that of the OGFC-1 specimen, but its splitting strength is higher. It can be seen that the splitting strength of the asphalt mixture increases with the increase of the void fractal dimension. It shows that there are certain shortcomings in evaluating the durability of OGFC mixtures by porosity index. When the porosity of the mixture is close, the splitting strength of the asphalt mixture is not only related to the porosity but also to its void structure, and the fractal dimension of the void can more effectively characterize the durability of the OGFC mixture specimen. The relationship between the fractal dimension of the void and the splitting strength is shown in Figure 11.

Fitting the relationship between the fractal dimension of the gap and the splitting strength, the relationship between the two is shown in (3):

$$R_T = -3.892 + 2.776D. \tag{3}$$

Here, R_T is the splitting strength and D is fractal dimension of voids.

The correlation coefficient of (3) is 0.996. Since $R_T > 0$, the value range of D is 1.4~2.

The study found that the main reason for the difference in the fractal dimension of voids is the proportion of voids larger than 3 mm in the asphalt mixture. Combining Figures 4–6, it can be seen that in the OGFC-1, OGFC-2, and OGFC-3 specimens, the proportions of the voids greater than 3 mm are 33%, 32%, and 37%, respectively. The data of this research show that the proportion of the voids larger than 3 mm is larger, the

fractal dimension of the voids is smaller. Therefore, the proportion of the voids larger than 3 mm has a great influence on the strength of OFGC mixture.

4. Conclusions

This paper uses CT technology to obtain the image information of the OGFC mixture specimen. On this basis, the void distribution characteristics of the OGFC mixture specimen are analyzed, and the corresponding relationship between the void distribution characteristics and the OGFC mixture damage is determined. The main conclusions are as follows:

(i) Based on MATLAB programming, calculating the void ratio by the number of pixels is an effective method, and the calculated void ratio is very close to the measured void ratio.

(ii) The internal voids of the OGFC mixture are unevenly distributed along the height of the specimen. The void ratio at both ends of the specimen is relatively large and gradually decreases from both ends to the middle. That is, the two ends of the mixture are distributed with a small number of large voids, and the middle is a large number of small voids.

(iii) The Gauss-Amp function was used to establish the frequency distribution function of the equivalent void diameter of the OGFC mixture, and the frequency distribution histogram of the equivalent void diameter was compared to determine that OGFC-2 was the best gradation.

(iv) Based on fractal geometry, the corresponding relationship between the void fractal dimension and splitting strength of OGFC mixture is established. The splitting strength increases with the increase of the void fractal dimension.

(v) The voids in the OGFC mixture with an equivalent diameter greater than 3 mm have a great influence on its splitting strength.

(vi) There is a positive linear relationship between the number of voids and the splitting strength. OGFC mixtures with more voids and relatively uniform void diameter distribution have better durability.

Data Availability

The data used to support the findings of this are available on request from the corresponding author.

Conflicts of Interest

The authors declare that they have no conflicts of interest.

References

[1] J. Zhang, "Research on asphalt mixture microstructure analysis method based on digital image processing technology," *Department of Road and Traffic Engineering*, Doctoral dissertation, Tongji University, Shanghai, China, 2000.

[2] L. I. Zhi, "Analysis of volume composition characteristics of asphalt mixture based on digital image processing technology," *Road and Railway Construction*, Doctoral Dissertation, Harbin Institute of Technology, Harbin, China, 2002.

[3] Q. Yao, "Research on Asphalt Mixture Composition Characteristics Based on Digital Image Processing Technology," Master's Thesis, Changan University, Xi'an, China, 2004.

[4] C. Wang, "Research on Asphalt Mixture Gradation Detection Technology Based on Digital Image," Master's Thesis, Changan University, Xi'an, China, 2007.

[5] Q. Zhang, Y. Bai, and D. Liang, "CT image entropy analysis for influences of moisture on asphalt mixtures," *J. Highway*, vol. 52, no. 4, pp. 158–161, 2007.

[6] Y. Hong, "Application and Research of Digital Image in Asphalt Mixture," Master's Thesis, Chongqing Jiaotong University, Chongqing, China, 2008.

[7] A. K. Apeagyei, J. R. A. Grenfell, and G. D. Airey, "Observation of reversible moisture damage in asphalt mixtures," *Construction and Building Materials*, vol. 60, pp. 73–80, 2014.

[8] D. L. Presti, N. A. Hassan, R. Khan, and G. Airey, "Reclaimed asphalt test specimen preparation assisted by image analysis," *Journal of Materials in Civil Engineering*, vol. 27, no. 8, 2014.

[9] M. Mohajeri, A. A. A. Molenaar, and M. F. C. V. D. Ven, "Experimental study into the fundamental understanding of blending between reclaimed asphalt binder and virgin bitumen using nanoindentation and nano-computed tomography," *Road Materials and Pavement Design*, vol. 15, no. 2, pp. 372–384, 2014.

[10] Z. A. Arega, A. Bhasin, and T. D. Kesel, "Influence of extended aging on the properties of asphalt composites produced using hot and warm mix methods," *Construction and Building Materials*, vol. 44, pp. 168–174, 2013.

[11] D. Braz, R. C. Barroso, R. T. Lopes, and L. M. G. Motta, "Crack detection in asphaltic mixtures by computed tomography," *NDT & E International*, vol. 44, no. 2, pp. 195–201, 2011.

[12] A. Moriyoshi, N. Takahashi, O. Ikeda, M. Kawashima, and T. Akabane, "Strain distribution in asphalt mixtures during the wheel tracking test at high temperatures," *Construction and Building Materials*, vol. 40, pp. 1128–1135, 2013.

[13] P. Liu, J. Hu, D. Wang et al., "Modelling and evaluation of aggregate morphology on asphalt compression behavior," *Construction and Building Materials*, vol. 133, pp. 196–208, 2017.

[14] J. Hu, P. Liu, and B. Steinauer, "A study on fatigue damage of asphalt mixture under different compaction using 3D-microstructural characteristics," *Journal of Frontiers of Structural and Civil Engineering*, vol. 11, pp. 1–9, 2017.

[15] J. Desrues, G. Viggiani, and P. Bésuelle, *X-ray Tomography as a Tool for Micromechanical Investigations of Cement and Mortar*, Wiley, NJ, USA, 2010.

[16] Y. M. Su, N. Hossiney, and M. Tia, "The analysis of air voids in concrete specimen using X-ray computed tomography," in *Nondestructive Characterization for Composite Materials,Aerospace Engineering, Civil Infrastructure, and Homeland Security*, T. Y. Yu, A. L. Gyekenyesi, P. J. Shull, A. A. Diaz, and H. F. Wu, Eds., SPIE, Bellingham, WA, USA, 2013.

[17] A. T. Papagiannakis, A. Abbas, and E. Masad, "Micromechanical analysis of viscoelastic properties of asphalt concretes, bituminous paving mixtures," *Materiales de Construcción*, vol. 1789, pp. 113–120, 2002.

[18] E. Masad, B. Muhunthan, N. Shashidhar, and T. Harman, "Internal structure characterization of asphalt concrete using image analysis," *Journal of Computing in Civil Engineering*, vol. 13, no. 2, pp. 88–95, 1999.

[19] M. Eyad and N. Somadevan, "Finite-element analysis of influence of localized strain distribution on asphalt mix properties," *Journal of Engineering Mechanics*, vol. 128, no. 10, pp. 1105–1114, 2002.

[20] E. Masad and J. Button, "Implications of experimental measurements and analyses of the internal structure of hot-mix asphalt," *Transportation Research Record: Journal of the Transportation Research Board*, vol. 1891, no. 1, pp. 212–220, 2004.

[21] E. Masad, A. Castelblanco, and B. Birgisson, "Effects of air void size distribution, pore pressure, and bond energy on moisture damage," *Journal of Testing and Evaluation*, vol. 34, no. 1, pp. 15–23, 2006.

[22] E. Masad and V. K. Jandhyala, "Characterization of air void distribution in asphalt mixes using X-ray computed tomography," *Journal of Materials in Civil Engineering*, vol. 14, no. 3, pp. 122–129, 2002.

[23] M. Eyad and J. W. Button, "Unified imaging approach for measuring aggregate angularity and texture," *J. Computer-Aided Civil and Infrastructure Engineering*, vol. 15, no. 4, pp. 273–280, 2010.

[24] A. C. Torres, *Probabilistic Analysis of Air Void Structure and its Relationship to Permeability and Moisture Damage of Hot Mix Asphalt*, Texas A&M University, Collage Station, TX, U.S.A, 2006.

[25] H. Xu, F. Chen, X. Yao, and Y. Tan, "Micro-scale moisture distribution and hydrologically active pores in partially saturated asphalt mixtures by X-ray computed tomography," *Construction and Building Materials*, vol. 160, pp. 653–667, 2018.

[26] J. Zhang, *Research on Characterization of Air Void Distribution and its fine Description in Porous Drainage Asphalt Mixture*, Chang'an University, Xi'an, China, 2008.

[27] L. Wen, *Research on Digital Image Processing Technology and Probability Statistics Method of Asphalt Mixture*, South China University of Technology, Guangzhou, China, 2009.

[28] E. Masad, L. Tashman, N. Somedavan, and D. Little, "Micromechanics-based analysis of stiffness anisotropy in asphalt mixtures," *Journal of Materials in Civil Engineering*, vol. 14, no. 5, pp. 374–383, 2002.

[29] G. Xu, "Characterization of air voids distribution in the open-graded asphalt mixture based on 2D image analysis," *Journal of Applied Sciences*, vol. 9, pp. 1–15, 2019.

[30] H. Xin, *Fractal Theory and Applications*, University of Science and Technology of China Press, Hefei, China, 1993.